Prepared for submission to JHEP

W^+W^- pair production in proton-proton collisions: small missing terms

Marta Łuszczak[a] **Antoni Szczurek**[a,b] **Christophe Royon**[c]

[a] *University of Rzeszów, PL-35-959 Rzeszów, Poland*
[b] *Institute of Nuclear Physics PAN, PL-31-342 Kraków, Poland*
[c] *IRFU/Service de Physique des Particules, CEA/Saclay, France*

E-mail: luszczak@univ.rzeszow.pl, antoni.szczurek@ifj.edu.pl, christophe.royon@cea.fr

Abstract: W^+W^- production is one of the golden channels for testing the Standard Model as well for searches beyond the Standard Model. We discuss many new subleading processes for inclusive production of W^+W^- pairs generally not included in the litterature so far. We focus mainly on photon-photon induced processes. We include elastic-elastic, elastic-inelastic, inelastic-elastic and inelastic-inelastic contributions. We also calculate the contributions with resolved photons including the partonic substructure of the virtual photon. Predictions for the total cross section and differential distributions in W- boson rapidity and transverse momentum as well as WW invariant mass are presented. The $\gamma\gamma$ components only constitute about 1-2 % of the inclusive W^+W^- cross section but increases up to about 10 % at large $W^\pm$ transverse momenta, and are even comparable to the dominant $q\bar{q}$ component at large M_{WW}, i.e. are much larger than the $gg \to W^+W^-$ one.

Keywords: Phenomenological Models, QCD Phenomenology

arXiv:1409.1803v1 [hep-ph] 5 Sep 2014

Contents

1 Introduction **1**

2 Processes leading to W pair production **2**
- 2.1 $\gamma\gamma \to W^+W^-$ reaction 2
- 2.2 Exclusive $pp \to ppW^+W^-$ reaction 3
- 2.3 Inclusive production of W^+W^- pairs 4
  - 2.3.1 $q\bar{q} \to W^+W^-$ mechanism 4
  - 2.3.2 $gg \to W^+W^-$ mechanism 5
  - 2.3.3 $pp \to W^+W^-X$ production via photon exchanges 5
  - 2.3.4 Single diffractive production of W^+W^- pairs 9
  - 2.3.5 Double parton scattering 12

3 Results **14**
- 3.1 Discussion of the photon induced inelastic contributions 14
- 3.2 Discussion of the contributions leading to $WW + X$ in the final state 15

4 Conclusions **21**

1 Introduction

The $pp \to W^+W^-X$ process is quite fundamental in particle physics. It constitutes an important, irreducible background to the observation of the Higgs boson in the W^+W^- channel and furthermore, can be used to test Standard Model gauge boson couplings and study them in models beyond the Standard Model.

Especially, the exclusive W^+W^- process is interesting by itself since it can be used to test the Standard Model and many beyond Standard Model theories. The photon-photon contribution was recently considered in the litterature [1, 2] and dominates at W pair masses. The exclusive QCD diffractive mechanism of central exclusive production of W^+W^- pairs (in which diagrams with intermediate virtual Higgs boson as well as quark box diagrams are included) was discussed in Ref. [3] and turned out to be small at high masses but dominating at low masses. The W^+W^- pair production signal is particularly sensitive to new Physics contributions in the $\gamma\gamma \to W^+W^-$ subprocess [1, 2]. Similar analysis has been considered recently for $\gamma\gamma \to ZZ$ and $\gamma\gamma \to \gamma\gamma$ [1, 5]. Corresponding measurements would be possible to perform at ATLAS or CMS provided the very forward proton detectors are installed [6].

In the present paper we concentrate on the inclusive and exclusive productions of W^+W^- pairs. The inclusive production of W^+W^- has been measured recently by the CMS and ATLAS collaborations [7, 8]. The total measured cross section by the CMS

collaboration is 41.1 ± 15.3 (stat) ± 5.8 (syst) ± 4.5 (lumi) pb, the total measured cross section using the ATLAS detector with slightly better statistics is 54.4 ± 4.0 (stat.) ± 3.9 (syst.) ± 2.0 (lumi.) pb. The ATLAS and CMS results are somewhat larger than the Standard Model predictions of 44.4 ± 2.8 pb [8]. The Standard Model predictions do not include several potentially important subleading processes, and this is the aim of this paper to compute the usually missing processes in the litterature leading to pairs of Ws in the final state.

In this paper, we review several processes which are usually ignored in the litterature and discuss if they could explain the slight discrepancy between the measurements and the usual SM predictions. Some of the not included processes were already discussed previously. One of such examples is the double parton scattering (DPS) that was discussed e.g. in Ref.[10–12]. The W^+W^- final states constitutes a background to the Higgs boson production.

In section II of the paper, we will review the different processes leading to two Ws in the final state and compute the production cross sections. We will discuss in turn the exclusive production of W pairs via photon and gluon exchanges, the inclusive one originating by quark and gluon exchanges, the inelastic-inelastic and elastic-inelastic productions, as well as the diffractive contributions. We thus include for the first time processes with resolved photons as well as single-diffractive production of W^+W^- pairs. In section III, we discuss the results and study how to measure each component individually.

2 Processes leading to W pair production

In this section, we review all processes leading to pairs of Ws in the final state.

2.1 $\gamma\gamma \to W^+W^-$ reaction

In this section, we discuss a basic ingredient to produce W pairs exclusively via photon exchanges. In the next section, we will convolute this elementary cross section with the photon flux originating from the protons.

Let us start from a reminder about the $\gamma\gamma \to W^+W^-$ coupling within the Standard Model. The three-boson $WW\gamma$ and four-boson $WW\gamma\gamma$ couplings, which contribute to the $\gamma\gamma \to W^+W^-$ process in the leading order read

$$\begin{aligned}\mathcal{L}_{WW\gamma} &= -ie(A_\mu W^-_\nu \overset{\leftrightarrow}{\partial^\mu} W^{+\nu} + W^-_\mu W^+_\nu \overset{\leftrightarrow}{\partial^\mu} A^\nu + W^+_\mu A_\nu \overset{\leftrightarrow}{\partial^\mu} W^{-\nu}),\\ \mathcal{L}_{WW\gamma\gamma} &= -e^2\left(W^-_\mu W^{+\mu} A_\nu A^\nu - W^+_\mu A^\mu W^-_\nu A^\nu\right),\end{aligned} \tag{2.1}$$

where the asymmetric derivative has the form $X \overset{\leftrightarrow}{\partial^\mu} Y = X\partial^\mu Y - Y\partial^\mu X$.

The relevant leading-order subprocess diagrams are shown in Fig. 1.

Within the Standard Model, the elementary tree-level cross section for the $\gamma\gamma \to W^+W^-$ subprocess can be written in the very compact form in terms of the Mandelstam variables (see e.g. Ref. [22])

$$\frac{d\hat{\sigma}}{d\Omega} = \frac{3\alpha^2\beta}{2\hat{s}}\left(1 - \frac{2\hat{s}(2\hat{s}+3m_W^2)}{3(m_W^2-\hat{t})(m_W^2-\hat{u})} + \frac{2\hat{s}^2(\hat{s}^2+3m_W^4)}{3(m_W^2-\hat{t})^2(m_W^2-\hat{u})^2}\right), \tag{2.2}$$

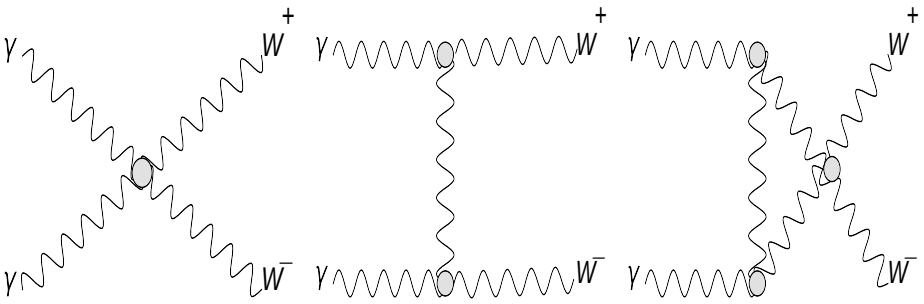

Figure 1. The leading order $\gamma\gamma \to W^+W^-$ subprocesses.

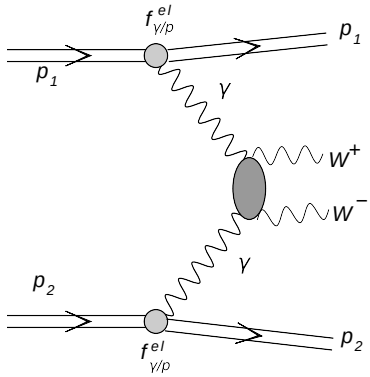

Figure 2. The general diagram for the $pp \to ppW^+W^-$ reaction via $\gamma\gamma \to W^+W^-$ subprocess.

where $\beta = \sqrt{1 - 4m_W^2/\hat{s}}$ is the velocity of the W bosons in their center-of-mass frame and the electromagnetic fine-structure constant $\alpha = e^2/(4\pi) \simeq 1/137$. The total elementary cross section can be obtained by integration of the differential cross section given above.

2.2 Exclusive $pp \to ppW^+W^-$ reaction

In this section, we give the exclusive WW production cross section via photon exchanges.

The $pp \to ppW^+W^-$ reaction is particularly interesting in the context of $\gamma\gamma WW$ coupling [1, 2]. The general diagram for the exclusive reaction is shown in Fig. 2.

In the Weizsäcker-Williams approximation, which was used so far in the litterature, the total cross section for the $pp \to pp(\gamma\gamma) \to W^+W^-$ can be written as in the parton model:

$$\sigma = \int dx_1 dx_2 \, f_1(x_1) \, f_2(x_2) \, \hat{\sigma}_{\gamma\gamma \to W^+W^-}(\hat{s}) \, . \tag{2.3}$$

We take the Weizsäcker-Williams equivalent photon fluxes f_1 and f_2 in protons from Ref. [23].

To calculate differential distributions the following parton formula can be conveniently used

$$\frac{d\sigma}{dy_+ dy_- d^2p_{W\perp}} = \frac{1}{16\pi^2 \hat{s}^2} \, x_1 f_1(x_1) \, x_2 f_2(x_2) \, \overline{|\mathcal{M}_{\gamma\gamma \to W^+W^-}(\hat{s}, \hat{t}, \hat{u})|^2} \, . \tag{2.4}$$

We shall not discuss here any approach beyond the Standard Model. A potentially interesting beyond Standard Model production of W^+W^- pairs due to the existence of extra-dimensions has been discussed previously e.g. in Refs. [1, 2].

The exclusive cross section could be also calculated more precisely in four-body calculations using the corresponding $2 \to 4$ matrix element. If exact exclusivity of the reaction is required then absorption effect related to soft proton-proton interactions has to be included. Such effects can be included consistently only in the four-body calculations but can be included only approximately in the Weizsacker-Williams approximation by multiplying the Born cross section by a given factor. From our experience in other $\gamma\gamma$ processes where four-body calculations were done this factor is about 0.8-0.9, that is of the order of 1, depending on the mass of the produced system. In the following, we assume this factor to be 1 and all cross sections should be multiplied by this factor once known.

2.3 Inclusive production of W^+W^- pairs

In this section, we discuss the inclusive production of W pairs. We first start by the usual production considered in the litterature via gluon and quark exchanges, We then describe new processes, starting by the W pair production via photon exchanges where we distinguish the elastic-elastic, elastic-inelastic and inelastic-inelastic contributions. We finish the section by studying the diffractive production of W pairs. All these contributions are "inclusive" in the sense that additional particles are produced together with the W pair.

The dominant contribution of W^+W^- pair production is initiated by quark-antiquark annihilation [22]. The gluon-gluon contribution to the inclusive cross section was calculated first in Ref. [24].

Therefore, for reference, we also consider the quark-antiquark and gluon-gluon components to the inclusive cross section. We briefly remind the basics for these well known dominant contributions.

2.3.1 $q\bar{q} \to W^+W^-$ mechanism

The generic diagram for the $q\bar{q}$ initiated processes is shown in Fig.3. This contains t- and u-channel quark exchanges as well as s-channel photon and Z-boson exchanges [22].

Therefore this process is also of interest as a probe of the gauge structure of the electroweak interactions. Relevant leading-order matrix element, averaged over quark colors and over initial spin polarizations and summed over final spin polarization, can be found e.g. in Ref. [25].

The corresponding differential cross section in leading-order approximation can be calculated as:

$$\frac{d\sigma}{dy_+ dy_- d^2p_{W\perp}} = \frac{1}{16\pi^2 \hat{s}^2} \sum_f [x_1 q_f(x_1,\mu^2)\, x_2 \bar{q}_f(x_2,\mu^2) + x_1 \bar{q}_f(x_1,\mu^2)\, x_2 q_f(x_2,\mu^2)] \overline{|\mathcal{M}_{q\bar{q}\to W^+W^-}(\hat{s},\hat{t},\hat{u})|^2}\,.$$

Above q_f and $\bar{q}_f$ are quark and antiquark distributions of a given flavor in the proton, x_1 and x_2 are corresponding longitudinal momentum fractions carried by the quark or antiquark and μ^2 is a QCD scale taken here to be $\mu^2 = m_t^2$, where m_t is the W-boson transverse mass.

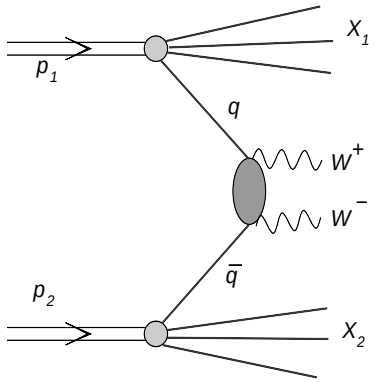

Figure 3. A generic diagram representing mechanisms for the production of W^+W^- pairs in the $q\bar{q} \to W^+W^-$ subprocess.

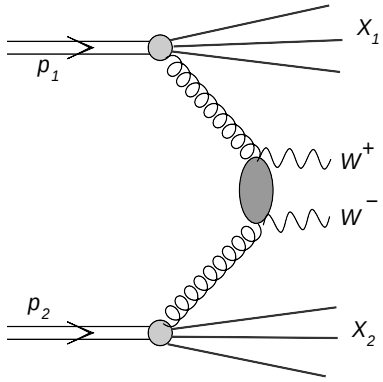

Figure 4. A generic diagram representing mechanisms for the production of W^+W^- pairs in the $gg \to W^+W^-$ subprocess.

2.3.2 $gg \to W^+W^-$ mechanism

The generic diagram for the gg initiated processes is shown in Fig.4. This contains both quark box diagrams and heavy-quark triangle with s-channel Higgs boson in the intermediate stage. More details of the relevant calculation can be found e.g. in Ref.[3].

The corresponding differential cross section corresponding to this contribution can be calculated as:

$$\frac{d\sigma}{dy_+ dy_- d^2p_{W\perp}} = \frac{1}{16\pi^2 \hat{s}^2}\, x_1 g(x_1,\mu^2)\, x_2 g(x_2,\mu^2) \overline{|\mathcal{M}_{gg\to W^+W^-}(\hat{s},\hat{t},\hat{u})|^2}\,, \qquad (2.5)$$

where g's are gluon distributions in the proton. This contribution is formally higher order in pQCD than the $q\bar{q}$ annihilation, but may be large numerically at higher energies when x_1 and x_2 become very small, i.e. gluon distributions are very large.

2.3.3 $pp \to W^+W^-X$ production via photon exchanges

In this section, we briefly discuss the inclusive $pp \to W^+W^-X$ mechanism via photon exchanges where we consider the cases when the protons are destroyed in the final state

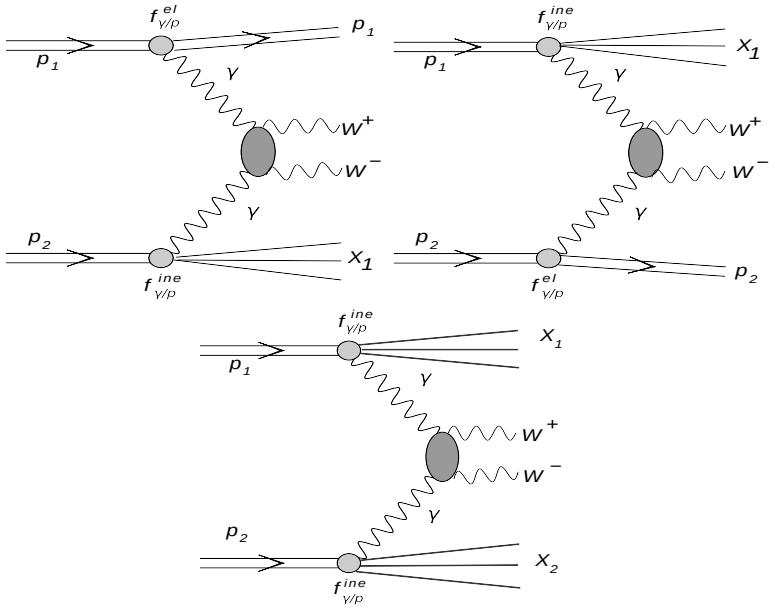

Figure 5. Diagrams representing inelastic photon-photon induced mechanisms for production of W^+W^- pairs.

(inelastic contributions) thus leading to a W pair and in addition the proton remnants. We calculate this contribution to the inclusive $pp \to W^+W^-X$ process for the first time in the litterature.

If at least one photon is a constituent of the nucleon, the mechanisms presented in Fig.5 are possible. In these cases at least one of participating protons does not survive the W^+W^- production process. In the following we consider two different approaches to the problem.

Naive approach to photon flux

Some $\gamma\gamma$ induced processes ($\gamma\gamma \to H^+H^-, L^+L^-$) were discussed long time ago in Ref.[26]. In these approaches the photon distribution in the proton is a convolution of the distribution of quarks in the proton and the distribution of photons in quarks/antiquarks

$$f_{\gamma/p} = f_q \otimes f_{\gamma/q} \, , \tag{2.6}$$

which can be written mathematically as

$$x f_{\gamma/p}(x) = \sum_q \int_x^1 dx_q f_q(x_q, \mu^2) e_q^2 \left(\frac{x}{x_q}\right) f_{\gamma/q}\left(\frac{x}{x_q}, Q_1^2, Q_2^2\right) \, , \tag{2.7}$$

where the sum runs over all quark and antiquark flavours. The flux of photons in a quark/antiquark in their approach was calculated as:

$$f_\gamma(z) = \frac{\alpha_{em}}{2\pi} \frac{1+(1-z)^2}{2} \log\left(\frac{Q_1^2}{Q_2^2}\right) \, . \tag{2.8}$$

The choice of the scales in the formulae is a bit ambigous. In these papers the authors have proposed the following set of scales:

$$\begin{aligned} Q_1^2 &= \max(\hat{s}/4 - m_W^2, 1\text{GeV}^2) \\ Q_2^2 &= 1\text{GeV}^2 \\ \mu^2 &= \hat{s}/4 \, . \end{aligned} \tag{2.9}$$

We use the approach decribed in this section as a reference for the formally more refined calculation described in the next subsection.

MRST-QED parton distributions

An improved approach how to include photons into inelastic processes was proposed some time ago by Martin, Roberts, Stirling and Thorne in Ref.[27]. In their approach the photon is treated on the same footing as quarks, antiquarks and gluons. Below we repeat the essential points of their formalism which includes combined QCD+QED evolution.

They proposed a QED-corrected evolution equations for the parton distributions of the proton [27]:

$$\begin{aligned} \frac{\partial q_i(x,\mu^2)}{\partial \log \mu^2} &= \frac{\alpha_S}{2\pi} \int_x^1 \frac{dy}{y} \Big\{ P_{qq}(y) \; q_i(\frac{x}{y},\mu^2) + P_{qg}(y) \; g(\frac{x}{y},\mu^2) \Big\} \\ &+ \frac{\alpha}{2\pi} \int_x^1 \frac{dy}{y} \Big\{ \tilde{P}_{qq}(y) \; e_i^2 q_i(\frac{x}{y},\mu^2) + P_{q\gamma}(y) \; e_i^2 \gamma(\frac{x}{y},\mu^2) \Big\}, \\ \frac{\partial g(x,\mu^2)}{\partial \log \mu^2} &= \frac{\alpha_S}{2\pi} \int_x^1 \frac{dy}{y} \Big\{ P_{gq}(y) \; \sum_j q_j(\frac{x}{y},\mu^2) + P_{gg}(y) \; g(\frac{x}{y},\mu^2) \Big\}, \\ \frac{\partial \gamma(x,\mu^2)}{\partial \log \mu^2} &= \frac{\alpha}{2\pi} \int_x^1 \frac{dy}{y} \Big\{ P_{\gamma q}(y) \; \sum_j e_j^2 \; q_j(\frac{x}{y},\mu^2) + P_{\gamma\gamma}(y) \; \gamma(\frac{x}{y},\mu^2) \Big\} \, , \end{aligned} \tag{2.10}$$

where

$$\begin{aligned} \tilde{P}_{qq} &= C_F^{-1} P_{qq}, \quad P_{\gamma q} = C_F^{-1} P_{gq}, \\ P_{q\gamma} &= T_R^{-1} P_{qg}, \quad P_{\gamma\gamma} = -\frac{2}{3} \sum_i e_i^2 \; \delta(1-y) \end{aligned}$$

The parton distributions in Eq.(2.10) fulfil the standard momentum sum rule:

$$\int_0^1 dx \; x \left\{ \sum_i q_i(x,\mu^2) + g(x,\mu^2) + \gamma(x,\mu^2) \right\} = 1 \, . \tag{2.11}$$

Cross section for photon-photon processes

At leading order, the corresponding triple differential cross section for inelastic-inelastic photon-photon contribution can be written as usually in the parton-model formalism:

$$\frac{d\sigma^{\gamma_{in}\gamma_{in}}}{dy_1 dy_2 d^2p_t} = \frac{1}{16\pi^2 \hat{s}^2} x_1\gamma_{in}(x_1,\mu^2) \; x_2\gamma_{in}(x_2,\mu^2) \; \overline{|\mathcal{M}_{\gamma\gamma\to W^+W^-}|^2} \, . \tag{2.12}$$

Above $\gamma_{in}(...)$ is used to denote "inelastic" photon distribution in the proton ($\gamma(...)$ in the previous section). $\gamma_{el}(...)$ will be reserved for purely elastic cases when proton stays intact.

The above contribution includes only cases when both nucleons do not survive the collision and nucleon debris are produced. The case when at least one nucleon survives the collision has to be considered separately. In this case one can include the corresponding photon distributions where an extra "el" index will be added. The corresponding contributions to the cross section can be then written as:

$$\frac{d\sigma^{\gamma_{in}\gamma_{el}}}{dy_1 dy_2 d^2p_t} = \frac{1}{16\pi^2\hat{s}^2} x_1\gamma_{in}(x_1,\mu^2)\; x_2\gamma_{el}(x_2,\mu^2)\; \overline{|\mathcal{M}_{\gamma\gamma\to W^+W^-}|^2}\;,$$

$$\frac{d\sigma^{\gamma_{el}\gamma_{in}}}{dy_1 dy_2 d^2p_t} = \frac{1}{16\pi^2\hat{s}^2} x_1\gamma_{el}(x_1,\mu^2)\; x_2\gamma_{in}(x_2,\mu^2)\; \overline{|\mathcal{M}_{\gamma\gamma\to W^+W^-}|^2}\;,$$

$$\frac{d\sigma^{\gamma_{el}\gamma_{el}}}{dy_1 dy_2 d^2p_t} = \frac{1}{16\pi^2\hat{s}^2} x_1\gamma_{el}(x_1,\mu^2)\; x_2\gamma_{el}(x_2,\mu^2)\; \overline{|\mathcal{M}_{\gamma\gamma\to W^+W^-}|^2}\;, \tag{2.13}$$

(2.14)

for inelastic-elastic, elastic-inelastic and elastic-elastic components, respectively. The last case was already discussed in a separate dedicated subsection. In the following the elastic photon fluxes are calculated using the Drees-Zeppenfeld parametrization [23], where a simple parametrization of the nucleon electromagnetic form factors is used. Such an approach is consistent with the partonic approach used recently to estimate the electroweak corrections to different QCD processes. The three terms shown above are usually omitted. In this paper we quantify these contributions for W^+W^- production.

Resolved photons

So far we have discussed direct photonic contributions. We also need to add the hadronic content of the photon. Asymmetric diagrams with one photon attached to the upper or lower proton, as shown in Fig.6, become possible. Extra photon remnant debris (called $X_{\gamma,1}$ or $X_{\gamma,2}$ in the figure) appear in addition. One may expect that such diagrams lead to quite asymmetric distributions in W boson rapidity with maxima in forward and/or backward directions.

Another type of diagrams with resolved photons is shown in Fig.7. We expect the contributions of the second set of diagrams to be rather small.

In the case of resolved photons, the "photonic" quark/antiquark distributions in a proton must be calculated first. This can be done as the convolution

$$f^{\gamma}_{q/p} = f_{\gamma/p} \otimes f_{q/\gamma} \tag{2.15}$$

which mathematically means:

$$x f^{\gamma}_{q/p}(x) = \int_x^1 dx_\gamma f_{\gamma/p}(x_\gamma,\mu_s^2)\left(\frac{x}{x_\gamma}\right) f\left(\frac{x}{x_\gamma},\mu_h^2\right)\;. \tag{2.16}$$

Technically the first $f_{\gamma/p}$ in the proton is computed on a dense grid for $\mu_s^2 \sim 1$ GeV^2 (virtuality of the photon) and it is used in the convolution formula (2.16). The second

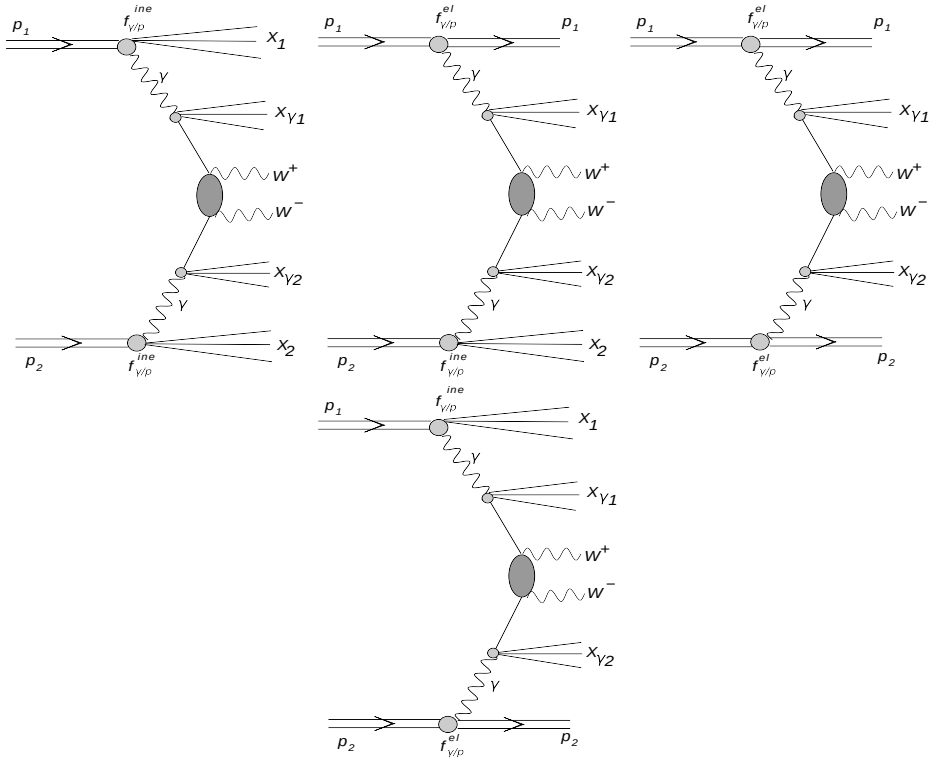

Figure 6. Diagrams representing some single resolved photon mechanisms with quark-antiquark annihilation for production of W^+W^- pairs. Similar diagrams with gluon-gluon subprocesses also exist.

scale is evidently hard $\mu_h^2 \sim M_{WW}^2$. The result strongly depends on the choice of the soft scale μ_s^2. In this sense our calculations are not very precise and must be treated rather as a rough estimate. The new quark/antiquark distributions of photonic origin are used to calculate the cross section as for the standard quark-antiquark annihilation subprocess.

2.3.4 Single diffractive production of W^+W^- pairs

Diffractive processes for W^+W^- production were not considered so far in the litterature but are potentially very important.

In the following we apply the resolved pomeron approach [28, 29]. In this approach one assumes that the Pomeron has a well defined partonic structure, and that the hard process takes place in Pomeron–proton or proton–Pomeron (single diffraction) or Pomeron–Pomeron (central diffraction) processes. The mechanism of single diffractive production of W^+W^- pairs is shown in Fig.8. We calculate the triple differential distributions

$$\frac{d\sigma_{SD}^{(1)}}{dy_1 dy_2 dp_t^2} = \sum_f \frac{\Big|M\Big|^2}{16\pi^2 \hat{s}^2} \Big[\Big(x_1 q_f^D(x_1,\mu^2)\, x_2 \bar{q}_f(x_2,\mu^2) \Big) + \Big(x_1 \bar{q}_f^D(x_1,\mu^2)\, x_2 q_f(x_2,\mu^2) \Big) \Big], \tag{2.17}$$

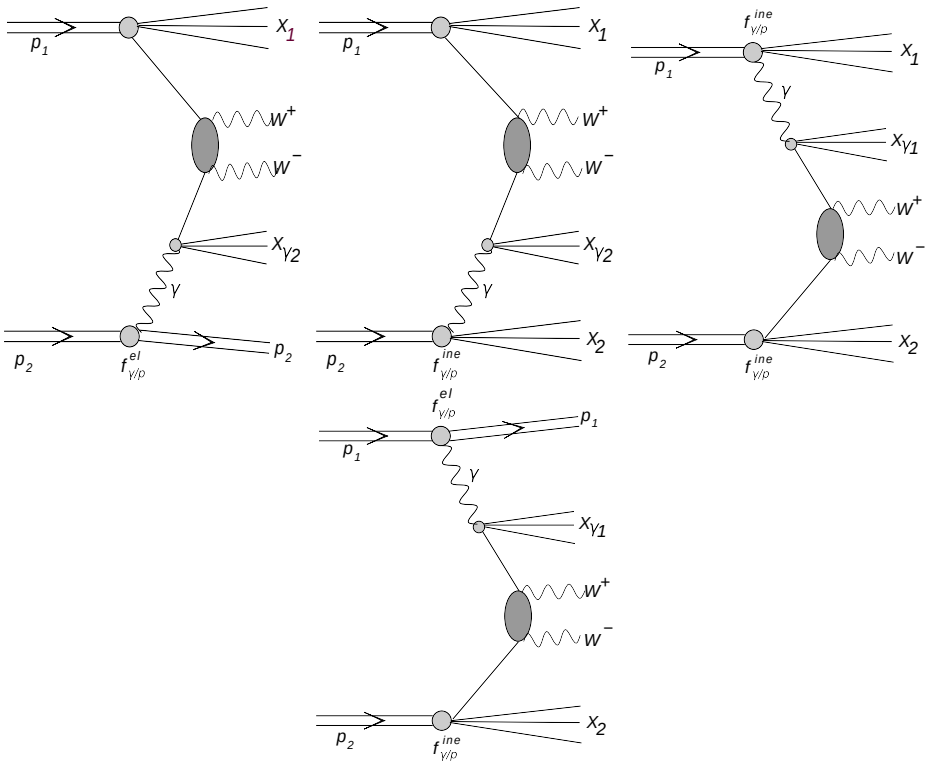

Figure 7. Diagrams representing mechanisms with two resolved photons for the production of W^+W^- pairs.

$$\frac{d\sigma^{(2)}_{SD}}{dy_1 dy_2 dp_t^2} = \sum_f \frac{\Big|M\Big|^2}{16\pi^2 \hat{s}^2} \Big[\Big(x_1 q_f(x_1,\mu^2)\, x_2 \bar{q}_f^D(x_2,\mu^2) \Big) + \Big(x_1 \bar{q}_f(x_1,\mu^2)\, x_2 q_f^D(x_2,\mu^2) \Big) \Big], \tag{2.18}$$

$$\frac{d\sigma_{CD}}{dy_1 dy_2 dp_t^2} = \sum_f \frac{\Big|M\Big|^2}{16\pi^2 \hat{s}^2} \Big[\Big(x_1 q_f^D(x_1,\mu^2)\, x_2 \bar{q}_f^D(x_2,\mu^2) \Big) + \Big(x_1 \bar{q}_f^D(x_1,\mu^2)\, x_2 q_f^D(x_2,\mu^2) \Big) \Big] \tag{2.19}$$

for single-diffractive and central-diffractive production, respectively. q_f^D and $\bar{q}_f^D$ are so - called diffractive quark and antiquark distributions, respectively. We shall return to them in the framework of the resolved pomeron model somewhat below. The matrix element squared for the $q\bar{q} \to W^+W^-$ process is the same as previously discussed for the non-diffractive processes.

In this approach longitudinal momentum fractions are calculated as

$$\begin{aligned} x_1 &= \frac{m_t}{\sqrt{s}} \Big(e^{y_2} + e^{y_2} \Big), \\ x_2 &= \frac{m_t}{\sqrt{s}} \Big(e^{-y_1} + e^{-y_2} \Big) \end{aligned} \tag{2.20}$$

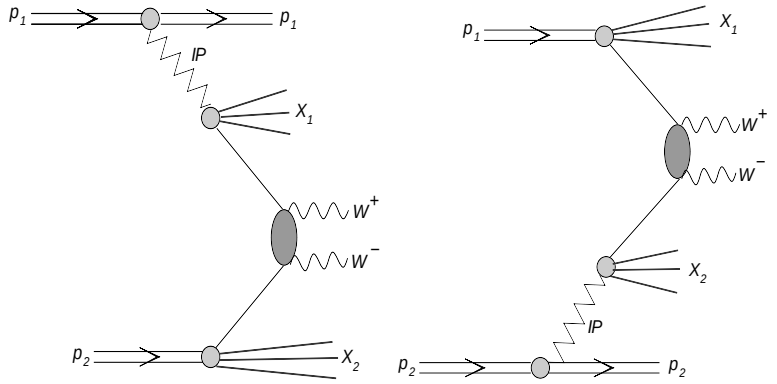

Figure 8. Diagrams representing single diffractive mechanism of production of W^+W^- pairs.

with $m_t = \sqrt{(p_t^2 + m_W^2)} \approx p_t$. The distribution in the WW invariant mass can be obtained by binning differential cross section in M_{WW}.

In the present analysis we consequently do not calculate higher-order contributions. In principle, they could be included effectively with the help of a so-called K-factor.

The "diffractive" quark/antiquark distribution of flavour f can be obtained by a convolution of the Pomeron flux $f_{I\!P}(x_{I\!P})$ and the parton distribution in the Pomeron $q_{f/I\!P}(\beta, \mu^2)$:

$$q_f^D(x,\mu^2) = \int dx_{I\!P} d\beta\, \delta(x - x_{I\!P}\beta) q_{f/I\!P}(\beta,\mu^2)\, f_{I\!P}(x_{I\!P}) = \int_x^1 \frac{dx_{I\!P}}{x_{I\!P}}\, f_{I\!P}(x_{I\!P}) q_{f/I\!P}(\frac{x}{x_{I\!P}},\mu^2)\,. \tag{2.21}$$

The Pomeron flux $f_{I\!P}(x_{I\!P})$ is integrated over the four–momentum transfer

$$f_{I\!P}(x_{I\!P}) = \int_{t_{min}}^{t_{max}} dt\, f(x_{I\!P}, t)\,, \tag{2.22}$$

with t_{min}, t_{max} being kinematic boundaries.

Both pomeron flux factors $f_{I\!P}(x_{I\!P}, t)$ and the quark/antiquark distributions in the pomeron are taken from the H1 collaboration analysis of diffractive structure function and diffractive dijets at HERA [30]. The factorization scale for diffractive parton distributions is taken here as $\mu^2 = m_t^2$.

In the present analysis we consider both pomeron and subleading reggeon contributions. In the H1 collaboration analysis the pion structure function was used for the subleading reggeons and the corresponding flux was fitted to the diffractive DIS data. The corresponding diffractive quark distributions are obtained by replacing the pomeron flux by the reggeon flux and the quark/antiquark distributions in the pomeron by their counterparts in subleading reggeon(s). Additional details can be found in [30]. In the case of pomeron exchange the upper limit in (2.21) is taken to be 0.1 and for reggeon exchange 0.2. In our opinion, the whole Regge formalism does not apply above these limits and therefore unphysical results could be obtained.

Up to now we have assumed Regge factorization which is known to be violated in hadron-hadron collisions. It is known that these are soft interactions which lead to an extra production of particles which fill in the rapidity gaps related to pomeron exchange.

If rapidity gap (gaps) is required (measured) then one has to include absorption effect in the formalism of the resolved pomeron/reggeon which can be interpreted as a probability of no extra soft interactions leading to the destruction of the rapidity gap.

Different models of absorption corrections (one-, two- or three-channel approaches) for diffractive processes were presented in the litterature. The absorption effects for diffractive processes were calculated e.g. in Ref [31, 32]. The different models give slightly different predictions. Usually an average value of the gap survival probability $< |S|^2 >$ is calculated first and the cross sections for different processes are multiplied by this value. We shall follow this somewhat simplified approach. Numerical values of the gap survival probability can be found in [31, 32]. The survival probability depends on the collision energy. It is sometimes parametrized as:

$$< |S|^2 > (\sqrt{s}) = \frac{a}{b + \ln(\sqrt{s})} \ . \tag{2.23}$$

The numerical values of the parameters can be found in original publications. At the LHC energy of 14 TeV one gets typically $S_G^2 = 0.03$. The diffractive cross sections at 8 TeV below will be multiplied by the gap survival factor $S_G^2 = 0.08$ extracted recently by the CMS collaboration [36] for diffractive dijet production. In our opinion there is about 30 % uncertainty on this value and it will be important to measure it using the incoming data at 13 TeV. In general, the absorptive corrections for single and central diffractive processes could be somewhat different.

2.3.5 Double parton scattering

For completeness we also consider the double parton scattering mechanism discussed already in the litterature but not included in the Standard Model predictions to the inclusive cross section and distributions. The diagram representating the double parton scattering process is shown in Fig.9.

The cross section for double parton scattering is often modelled in the factorized anzatz which in our case would mean:

$$\sigma_{W^+W^-}^{DPS} = \frac{1}{\sigma_{qq}^{eff}} \sigma_{W^+} \sigma_{W^-} \ . \tag{2.24}$$

This is a rather effective approach assuming implicitly the lack of parton correlations. In principle also single parton splitting mechanisms should be included explicitly (see e.g. [33]). The phenomenological formula includes them effectively.

In general, the parameter σ_{qq} does not need to be the same as for gluon-gluon initiated processes, which is better known phenomenologically ($\sigma_{gg}^{eff} \approx 15$ mb) from analyses of different experimental data. In the present, rather conservative, calculations we take it to be $\sigma_{qq}^{eff} = \sigma_{gg}^{eff} = 15$ mb. The latter value is known within about 10 % from systematics of gluon-gluon initiated processes at the Tevatron and LHC.

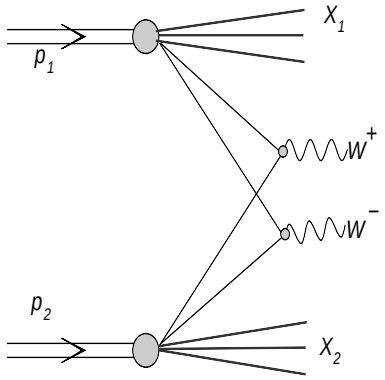

Figure 9. Diagram representing double parton scattering mechanism of production of W^+W^- pairs.

The factorized model (2.24) can be generalized to more differential distributions (see e.g. [34, 35]). For example in our case of W^+W^- production the cross section differential in W boson rapidities can be written as:

$$\frac{d\sigma^{DPS}_{W^+W^-}}{dy_+ dy_-} = \frac{1}{\sigma^{eff}_{qq}} \frac{d\sigma^+_W}{dy_+} \frac{d\sigma^-_W}{dy_-} \ , \tag{2.25}$$

where y_+ and y_- are rapidites of W^+ and W^-, respectively. In particular, in leading-order approximation the cross section for quark-antiquark annihilation reads:

$$\frac{d\sigma}{dy} = \sum_{ij} \left(x_1 q_{i/1}(x_1,\mu^2) x_2 \bar{q}_{j/2}(x_2,\mu^2) + x_1 \bar{q}_{i/1}(x_1,\mu^2) x_2 q_{j/2}(x_1,\mu^2) \right) \overline{|\mathcal{M}_{ij\to W^\pm}|^2} \ , \tag{2.26}$$

where the matrix element for quark-antiquark annihilation to W bosons ($\mathcal{M}_{ij\to W^\pm}$) contains the Cabibbo-Kobayashi-Maskawa matrix elements. In the present paper we show the $\frac{d\sigma}{dy_+ dy_-}$ cross section, as well as the distributions in rapidity difference between W^+ and W^- and in M_{WW}. In the approximations made here (leading order approximation, no transverse momenta of W bosons)

$$M^2_{WW} = 2M^2_W \left(1 + \cosh(y_1 - y_2)\right) \ . \tag{2.27}$$

When calculating the cross section for single W boson production in leading-order approximation a well known Drell-Yan K-factor could be included. The double-parton scattering would be then multiplied by K^2. The K-factor for W^+ or W^- production is only slightly larger then 1 and in the consequence also K^2 is not far from 1.

Fast progress in understanding multi-parton interactions was achieved recently. It is clear at present that in addition to the ususal DPS terms, the perturbative parton splitting mechanism has to be included explicitly [14, 15]. The contribution of this mechanism can be as large as the conventional DPS contribution. This formalism contains, however, more partonic form factors that are not well known phenomenologically. We think that the estimate of the DPS effect based on the factorized Ansatz with empirical σ_{eff} can be

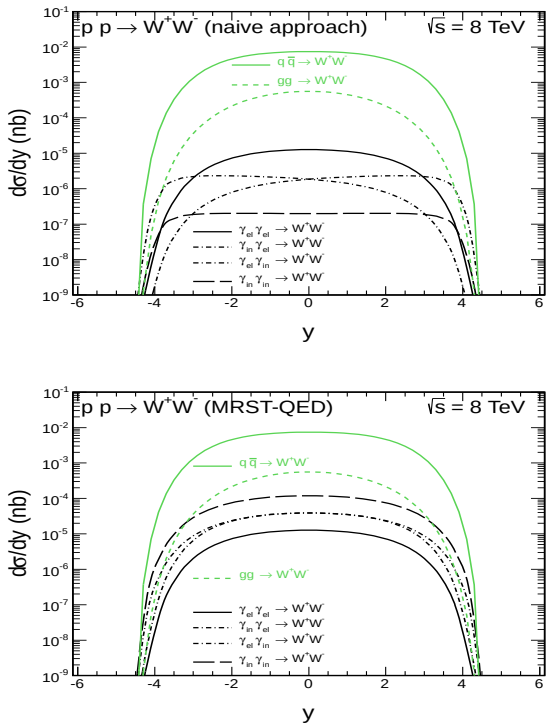

Figure 10. Rapidity distribution of W bosons for $\sqrt{s} = 8$ TeV. The left panel shows the results for the naive approach often used in the litterature, while the right panel shows the result with the QCD improved method proposed in Ref.[27].

better, at least in the moment. Further studies are needed also here. It is not easy to estimate the uncertainty of the so calculate DPS cross sections but we expect that the order of magnitude should be correct.

3 Results

In this section, we evaluate each contribution decribed in Section II and try to see if they can be measured experimentally in some dedicated kinematical regions.

3.1 Discussion of the photon induced inelastic contributions

Before a detailed survey of results of the different contributions discussed in the present paper, let us concentrate on some technical details concerning inelastic photon-photon contributions. In Fig.10 we show the rapidity distributions for the naive (left panel) and QCD improved (right panel) approaches discussed in section II. While in the naive approximation the elastic-elastic component is the largest and inelastic-inelastic is the smallest, in the QCD improved approach the situation is reversed, which shows the importance to use the complete approach and not the naive one. Here, in the QCD improved calculations $\mu_F^2 = m_t^2$ was used as the factorization scale.

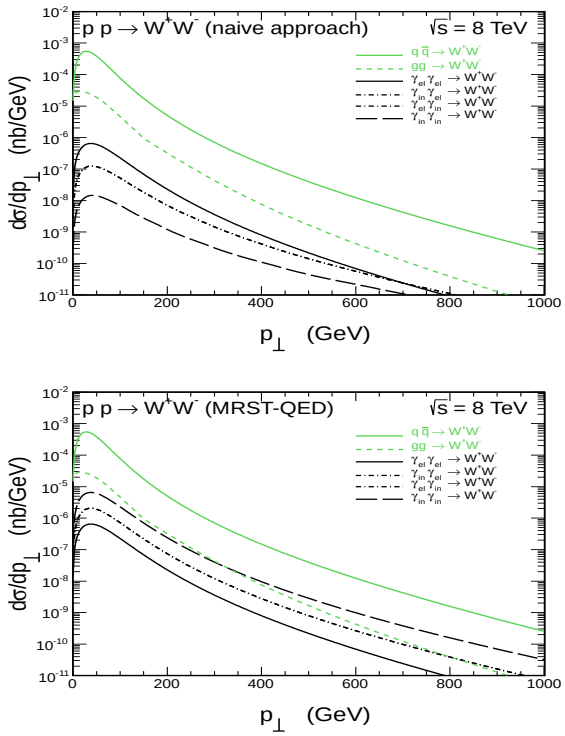

Figure 11. Transverse momentum distribution of W bosons for $\sqrt{s} = 8$ TeV. The left panel shows results for the naive approach often used in the past, while the right panel shows the result with the QCD improved method proposed in Ref.[27].

Concerning the searches of anomalous $\gamma\gamma WW$ coupling without proton tagging as performed by the D0 and CMS collabrations, the ratios of the inelastic-inelastic, elastic-inelastic and inelastic-elastic contribution to the elastic-elastic one are fundamental. In Fig.12 and 13 we show such ratios in W boson rapidity and transverse momentum. In the naive approach the ratios are smaller than 1 except for some small corners of the phase-space. In the QCD improved approach the ratios become much larger. In particular, the ratio for inelastic-inelastic contribution is one order of magnitude larger than 1, showing the importance of tagging the intact protons in the final state in order to measure the WW exclusive cross section.

3.2 Discussion of the contributions leading to $WW + X$ in the final state

In this section, we present a systematic survey of all the contributions discussed in the present paper.

The W boson rapidity distribution is shown in Fig.14. We show the separate contributions discussed in the present paper. The diffractive contribution is an order of magnitude larger than the resolved photon contribution. The estimated reggeon contribution is of similar size as the pomeron contribution. The y distributions of W^+ and W^- for double-parton scattering contribution are different and, in the approximation discussed here, have

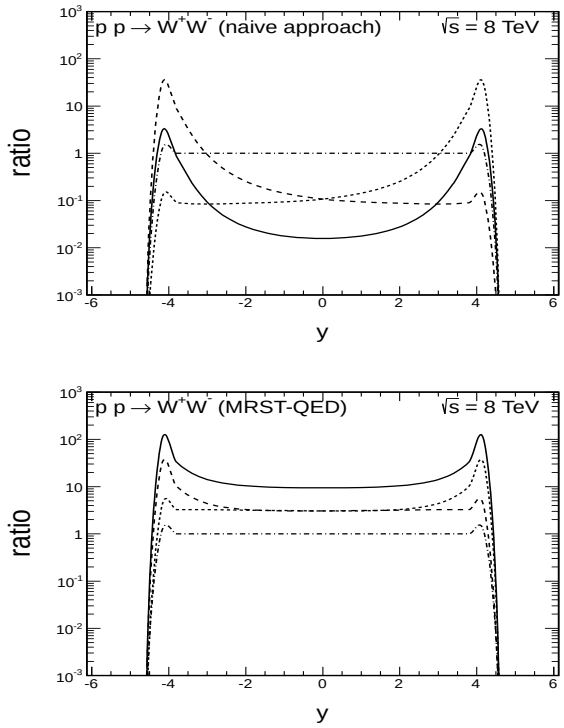

Figure 12. Ratio of elastic-inelastic (dashed), inelastic-elastic (dotted), inelastic-inelastic (dash-dotted) and all inelastic (solid) to the elastic-elastic cross section as a function of the W boson rapidity in the naive (left panel) and QCD improved (right panel) approaches.

identical shapes as for single production of W^+ and W^-, respectively. It would be therefore interesting to obtain experimentally separate distributions for W^+ and W^-. This is, however, a rather difficult task. The distributions of charged leptons (electrons, muons) could also be interesting in this context. It is also worth noticing that the relative size of each contribution will strongly depend on the mass of the W pair.

In Fig.15 we present the distributions in transverse momentum of the W bosons. All photon-photon components have rather similar shapes. The photon-photon contributions are somewhat harder (less steep) than those for diffractive and resolved photon mechanisms.

In Fig.16 we show the distributions in invariant mass of the W pairs. The relative contributions of the photon-photon and DPS components grow with the invariant mass. The same conclusion is true for the distribution in the rapidity distance between the gauge bosons. Experimentally, one rather measures the charged leptons than W bosons. Measuring the distributions in invariant mass of positive and negative leptons or in rapidity distance between them would be interesting.

Finally, in Fig.17 we present some interesting examples of two-dimensional distributions in W^+ and W^- rapidity. We show three different distributions for the dominant $q\bar{q}$, inelastic-inelastic photon-photon and double-parton scattering components. The $q\bar{q}$ component dominates at $y_1, y_2 \approx 0$. The photon-photon component has "broader" distribution

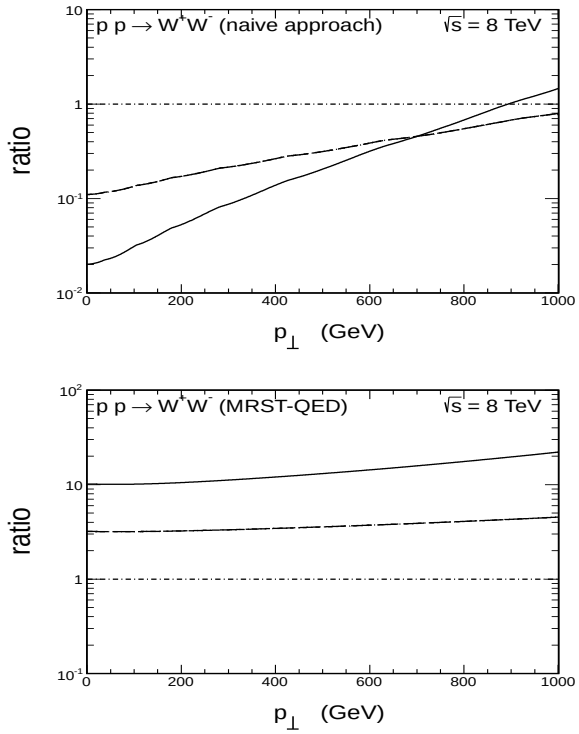

Figure 13. Ratio of elastic-inelastic (dashed), inelastic-elastic (dotted), inelastic-inelastic (dash-dotted) and all inelastic (solid) to the elastic-elastic cross section as a function of the W boson transverse momentum in the naive (left panel) and QCD improved (right panel) approaches.

in y_1 and y_2. In contrast, the double-parton scattering component gives a very flat two-dimensional distribution. The information presented in the figure can be used in order to "enhance" each component. The study of the lepton rapidity from the W-boson decays would be a next interesting step.

The results are summarized in Table 1. The photon-photon induced processes give quite large contribution. The single-resolved photon contributions are at least one order of magnitude smaller than the diffractive one. This is still surprisingly large. The reason that the single resolved photon contributions are relatively large is due to the fact that quark or antiquark carry on average a fairly large fraction of the photon longitudinal momentum. The double parton scattering contribution is small. It may be, however, important for large rapidity distances between gauge bosons. The diffractive contributions in the table are multiplied by the gap survival factor (S_G^2) which is known only approximately. The cross section of the additional processes usually not considered in the litterature are thus not enough to explain the discrepancy between data and theoretical calculations. New data at 14 TeV will be of considerable interest to know if this discrepancy is real.

In real experiments only a rather limited part of the phase space is covered. The total cross section is then obtained by extrapolating into unmeasured region with the help of Monte Carlo codes. It is needless to say that none of the new contributions discussed here

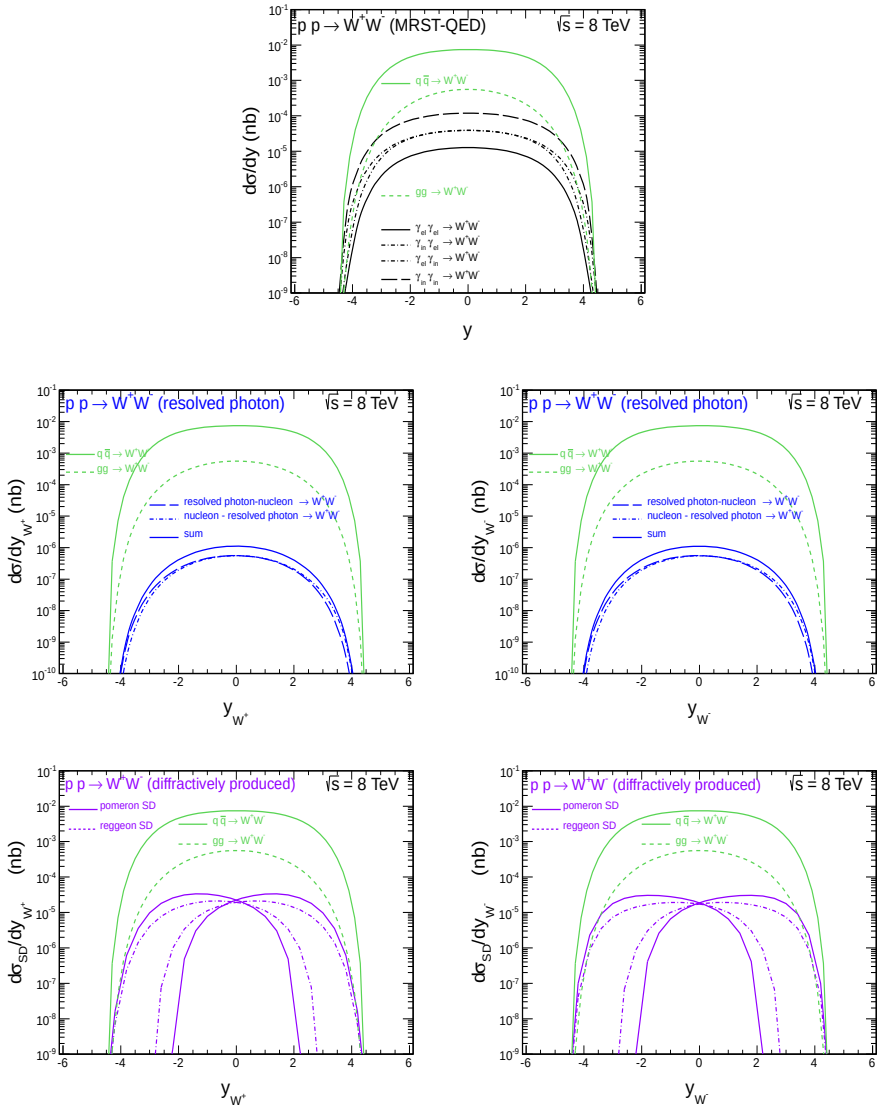

Figure 14. W boson rapidity distribution for $\sqrt{s} = 8$ TeV. The top panel shows contributions of all photon-photon induced processes as a function of y, the middle panels resolved photon contributions and the bottom panels distributions of the diffractive contribution. The diffractive cross section has been multiplied by the gap survival factor $S_G^2 = 0.08$ as needed for requirement of rapidity gaps.

is included when extrapolating purely experimental results to the phase-space integrated cross sections. This means that the "measured" total cross section is underestimated. Answering the question "by how much" requires dedicated Monte Carlo analyses.

Some comments on recent studies on $\gamma\gamma W^+W^-$ boson couplings, as performed recently by the D0 and CMS collaborations [16, 17] are in order. In the D0 collaboration analysis the inelastic contributions are not included when extracting limits on anomalous couplings, that lead to conservative limits. The CMS collaboration requires an extra condition of no

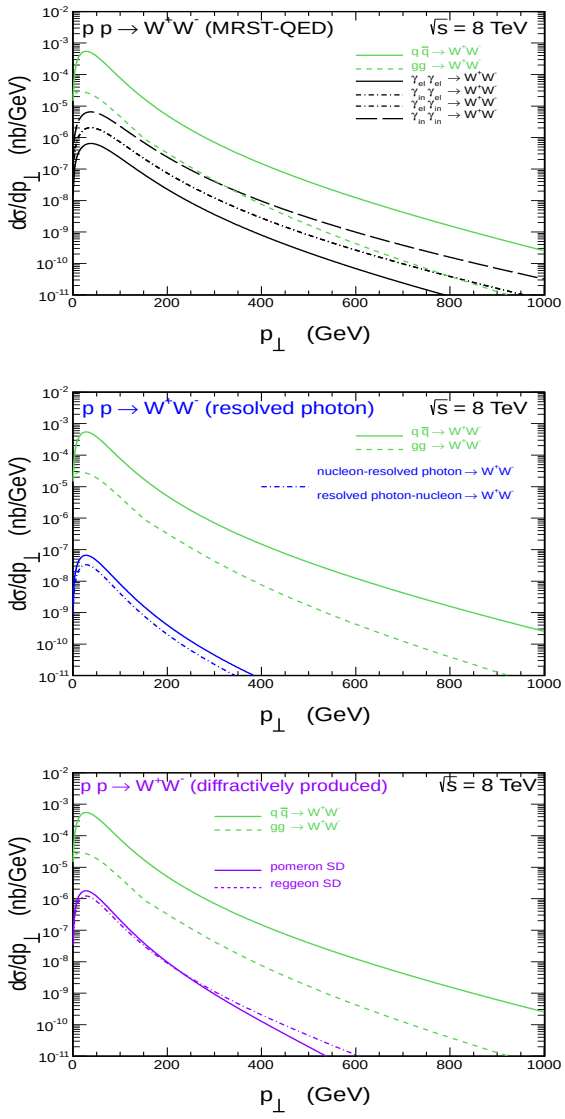

Figure 15. W boson transverse momentum distribution for $\sqrt{s} = 8$ TeV. The left-top panel shows all photon-photon induced processes, the right-top panel resolved photon contributions and the bottom panel the diffractive contribution. The diffractive cross section has been multiplied by the gap survival factor $S_G^2 = 0.08$. The distributions are of similar shape except for the $\gamma\gamma$ one which is slightly harder.

charged particles in the central pseudorapidity interval. When comparing calculations to the experimental data the inelastic contributions are estimated by rescaling the elastic-e lastic contribution by an experimental function depending on kinematical variables (invariant mass, transverse momentum of the $\mu^+\mu^-$ pair) obtained in the analysis of the $\mu^+\mu^-$ continuum. It is not clear to us whether such a procedure is consistent for W^+W^- production, where leptons come from the decays of the gauge bosons and the invariant mass

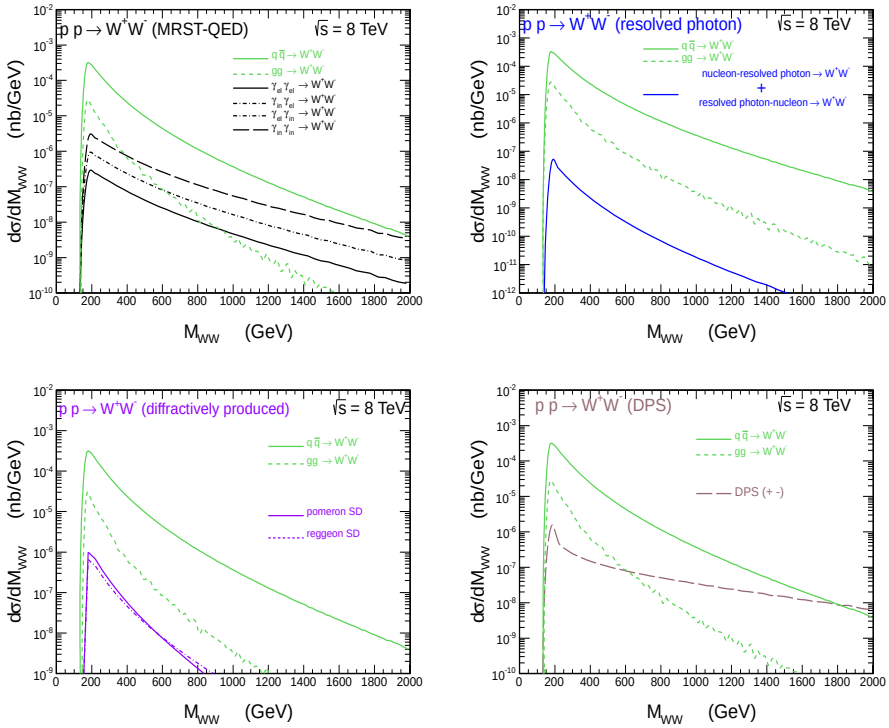

Figure 16. WW invariant mass distribution for $\sqrt{s} = 8$ TeV. The top-left panel shows contributions of all photon-photon induced processes, the top-right panel resolved photon contributions, the bottom-left panel the contributions of diffractive processes and the bottom-right panel the DPS contribution. The diffractive cross section has been multiplied by the gap survival factor $S_G^2 = 0.08$. The $\gamma\gamma$ contribution is larger at large masses than the DPS one.

and transverse momentum of the W^+W^- pair is very different than the invariant mass and transverse momentum of the corresponding dimuons. This cannot be checked in the present approach with collinear photons and requires the inclusion of photon transverse momenta. Within the present approach we predict that the inelastic $\gamma\gamma$ contributions are significantly larger than the elastic-elastic one. The fragmentation of the remnants of the inelastic excitations is needed to understand to which extent the inelastic contributions survive the veto condition. One can expect that particles from the fragmentation of the proton remnants after photon emission are emitted in rather forward/backward directions. The $D0$ collaboration also neglects the inelastic contribution when calculating the Standard Model background at large lepton transverse momenta, despite they have no explicit veto condition on charged particles. The diffractive contributions could also contribute to the distributions measured by the CMS and D0 collaborations. Clearly further analyses that focus on final states of proton remnants (after photon emission) are necessary.

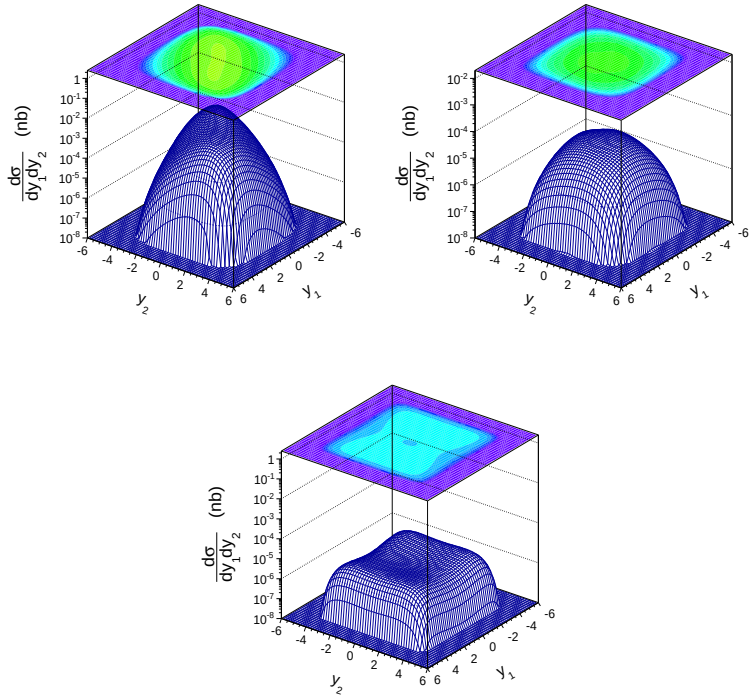

Figure 17. Two-dimensional distributions in rapidity of W^+ and rapidity of W^- for the dominant $q\bar{q}$ (left), inelastic-inelastic photon-photon (middle) and double-parton scattering (right) contributions at $\sqrt{s} = 8$ TeV.

4 Conclusions

In the present paper we discussed several contributions not considered traditionally in the so-called Standard Model predictions such as: photon-photon induced processes, processes with resolved photons, single and central diffractive processes and double parton scattering.

We have calculated for the first time the complete set of photon-photon and resolved photon-(anti)quark and (anti)quark-resolved photon contributions to the inclusive production of W^+W^- pairs. The photon-photon contributions can be classified into four topological categories: elastic-elastic, elastic-inelastic, inelastic-elastic and inelastic-inelastic, depending whether the proton(s) survives the emission of the photon or not. The elastic-inelastic and inelastic-elastic contributions were calculated for the first time in this study. The photon-photon contributions were calculated as in previous studies. for production of pairs of charged Higgs bosons or pairs of heavy leptons beyond the Standard Model, and within QCD-improved method using the MRST(QED) parton distributions. The second approach was already applied to the production of Standard Model charged lepton pair production and $c\bar{c}$ production. In the more refined approach we got $\sigma_{ela,ela} < \sigma_{ela,ine} = \sigma_{ine,ela} < \sigma_{ine,ine}$. In the approach when photon distribution in the proton undergoes QCD $\otimes$ QED evolution, the inelastic-inelastic contribution is the largest

contribution	1.96 TeV	7 TeV	8 TeV	14 TeV	comment
CDF	12.1 pb				
D0	13.8 pb				
ATLAS		54.4 pb			large extrapolation
CMS		41.1 pb			large extrapolation
$q\bar{q}$	9.86	27.24	33.04	70.21	dominant (LO, NLO)
gg	$5.17\ 10^{-2}$	1.48	1.97	5.87	subdominant (NLO)
$\gamma_{el}\gamma_{el}$	$3.07\ 10^{-3}$	$4.41\ 10^{-2}$	$5.40\ 10^{-2}$	$1.16\ 10^{-1}$	new, anomalous $\gamma\gamma WW$
$\gamma_{el}\gamma_{in}$	$1.08\ 10^{-2}$	$1.40\ 10^{-1}$	$1.71\ 10^{-1}$	$3.71\ 10^{-1}$	new, anomalous $\gamma\gamma WW$
$\gamma_{in}\gamma_{el}$	$1.08\ 10^{-2}$	$1.40\ 10^{-1}$	$1.71\ 10^{-1}$	$3.71\ 10^{-1}$	new, anomalous $\gamma\gamma WW$
$\gamma_{in}\gamma_{in}$	$3.72\ 10^{-2}$	$4.46\ 10^{-1}$	$5.47\ 10^{-1}$	1.19	anomalous $\gamma\gamma WW$
$\gamma_{el,res} - q/\bar{q}$	$1.04\ 10^{-4}$	$2.94\ 10^{-3}$	$3.83\ 10^{-3}$	$1.03\ 10^{-2}$	new, rather sizeable
$q/\bar{q} - \gamma_{el.res}$	$1.04\ 10^{-4}$	$2.94\ 10^{-3}$	$3.83\ 10^{-3}$	$1.03\ 10^{-2}$	new, rather sizeable
$\gamma_{in,res} - q/\bar{q}$					not calculated
$q/\bar{q} - \gamma_{in.res}$					not calculated
DPS(++)	$0.61\ 10^{-2}/2$	0.22/2	0.29/2	1.02/2	not included in NLO
DPS(- -)	$0.58\ 10^{-2}/2$	$0.76\ 10^{-1}/2$	0.11/2	0.40/2	not included in NLO
DPS(+-)	$0.6\ 10^{-2}$	0.13	0.18	0.64	not included in NLO
DPS(-+)	$0.6\ 10^{-2}$	0.13	0.18	0.64	not included in NLO
$\mathbb{P}p$ ($x_{\mathbb{P}} < 0.1$)	$0.28\ 10^{-2}$	$0.79\ 10^{-1}$	0.11	0.27	new, relatively large
$p\mathbb{P}$ ($x_{\mathbb{P}} < 0.1$)	$0.28\ 10^{-2}$	$0.79\ 10^{-1}$	0.11	0.27	new, relatively large
$\mathbb{R}p$ ($x_{\mathbb{R}} < 0.2$)	$0.45\ 10^{-2}$	$0.57\ 10^{-1}$	$0.72\ 10^{-1}$	0.18	new, relatively large
$p\mathbb{R}$ ($x_{\mathbb{R}} < 0.2$)	$0.45\ 10^{-2}$	$0.57\ 10^{-1}$	$0.72\ 10^{-1}$	0.18	new, relatively large
all subleading contributions	$8.87\ 10^{-2}$	1.31	1.68	4.25	

Table 1. Contributions of different subleading processes discussed in the present paper to the $WW + X$ cross section for different energies. The cross section is given in pb. The diffractive contributions have been multiplied by the gap survival factors: 0.1 at 1.96 TeV, 0.08 at 7 and 8 TeV (see [36]) and 0.03 at 14 TeV. The combinatorial factor 1/2 is shown explicitly for the double parton scattering (DPS) contribution for W^+W^+ and W^-W^- final states shown for completeness.

out of the four contributions. This shows that including photon into evolution equation is crucial. This includes also some processes beyond the Standard Model mentioned in this paper.

The inelastic contributions sum up to the cross section of the order of 0.5 - 1 pb at the LHC energies. The photon-photon contributions are particularly important at large WW invariant masses, i.e. probably also large invariant masses of charged leptons where its contribution is larger than that for gluon-gluon fusion.

The elastic-inelastic or inelastic-elastic contributions are interesting by themselves. Since they are related to the emission of forward/backward protons they could be potentially measured in the future with the help of forward proton detectors. Both CMS and ATLAS have plans for installing such detectors after the present (2013-2014) shutdown. Unfortunately the elastic-inelastic mechanisms are expected to have similar topology of the

final state as single-diffractive contributions to W^+W^- production. It would be therefore valuable to make a dedicated stu dy how to pin down the mixed elastic-inelastic contributions. Clearly this would be a valuable test of both the presented formalism and our understanding of the underlying reaction mechanism.

We have also discussed briefly the double-scattering mechanism which also significantly contributes to large M_{WW} invariant masses, the region where beyond Standard Model processes can be expected. The DPS was suggested recently as an important ingredient for the Higgs background in the WW^* or ZZ^* final channels. Our estimate is more than order of magnitude smaller than the one suggested recently in the litterature in order to explain the Higgs signal in the W^+W^- channel. However, the DPS calculation contains some phenomenological ingredients which are not fully understood.

Summarizing, we have shown that the omitted so far processes can contribute a few pb at $\sqrt{s} = 8$ TeV to the inclusive W^+W^- production cross section. There are even larger than at 14 TeV. The contribution of the subleading processes is growing faster with increasing center of mass energy than the standard Standard Model contributions (see the last row in the table). As discussed in our paper a precise estimation of contribution of these, also Standard Model, processes is rather difficult and requires further work. Some of the contributions discussed here have specific final state topology with one forward/backward proton separated in rapidity. Measuring the final state would therefore help to identify elastic-inelastic (inelastic elastic) two-photon contributions. Also single-diffractive contribution should have similar topology. They should have, however different dependence on t (four-momentum transfer squared).

After this paper was completed we have learned about a detailed study of uncertainties of a photon PDF in the framework of so-called neural network PDFs [37]. This analysis suggests that inelastic photon-induced contributions may have rather big uncertainies. The issue should be better clarified in the future by comparing similar calculation for two-photon-induced $\mu^+\mu^-$ production at large invariant masses of dileptons to appropriate experimental data.

Acknowledgments

We are indebted to Krzysztof Piotrzkowski, Jonathan Hollar, and Gustavo da Silveira for a discussion of the CMS experiment on semi-exclusive production of W^+W^- pairs. The help of Piotr Lebiedowicz in calculating the gluon-gluon component is acknowleded. We are indebted to Wolfgang Schäfer for a FORTRAN routine and an interesting discussion. We are indebted to Stefano Forte and Juan Rojo for a communication on their recent work on photon NNPDF. This work was partially supported by the Polish NCN grants: DEC-2011/01/B/ST2/04535 and DEC-2013/09/D/ST2/03724 and by the bilateral exchange program between Polish Academy of Sciences and FNRS, Belgium.

References

[1] O. Kepka and C. Royon, *Anomalous WW γ coupling in photon-induced processes using forward detectors at the LHC*, *Phys. Rev.* **D78** (2008) 073005;
E. Chapon, C. Royon and O. Kepka, *Anomalous quartic WW$\gamma\gamma$, ZZ$\gamma\gamma$, and trilinear WWγ couplings in two-photon processes at high luminosity at the LHC*, *Phys. Rev.* **D81** (2010) 074003;
S. Fichet, G. von Gersdorff, O. Kepka, B. Lenzi, C. Royon, M. Saimpert, *Probing new physics in diphoton production with proton tagging at the Large Hadron Collider*, *Phys. Rev. D* **89** (2014) 114004.

[2] N. Schul and K. Piotrzkowski, *Detection of two-photon exclusive production of supersymmetric pairs at the LHC*, *Nucl. Phys. B* (Proc. Suppl.) **179-180** (2008) 289;
T. Pierzchała and K. Piotrzkowski, *Sensitivity to anomalous quartic gauge couplings in photon-photon interactions at the LHC*, *Nucl. Phys. B* (Proc. Suppl.) **179-180** (2008) 257.

[3] P. Lebiedowicz, R. Pasechnik and A. Szczurek, *QCD diffractive mechanism of exclusive W^+W^- pair production at high energies*, *Nucl. Phys.* **B867** (2013) 61.

[4] S. Heinemeyer *et al.*, *Studying the MSSM Higgs sector by forward proton tagging at the LHC*, *Eur. Phys. J.* **C53** (2008) 231.

[5] R.S. Gupta, *Probing quartic neutral gauge boson couplings using diffractive photon fusion at the LHC*, *Phys. Rev.* **D85** (2012) 014006.

[6] CMS and TOTEM diffractive and forward physics working group, CERN/LHCC 2006-039/G-124, CMS Note 2007/002, TOTEM Note 06-5, December 2006;
M. Albrow et al. (FP420 R and D Collaboration), *The FP420 R and D Project: Higgs and New Physics with forward protons at the LHC*, JINST **4** (2009) T10001 [arXiv:0806.0302 [hep-ex]];
ATLAS Collaboration, *The AFP project in ATLAS, Letter of Intent of the PhaseI Upgrade*, http://cdsweb.cern.ch/record/1402470;
C. Royon (RP220 Collaboration), *Project to install roman pot detectors at 220 m in ATLAS*, arXiv:0706.1796 [physics.ins-det];
M. Tasevsky, *Diractive physics program in ATLAS experiment*, *Nucl. Phys. Proc. Suppl.* **179-180** (2008) 187;
The PPS upgrade project in CMS, M. Albrow, AIP Conf. Proc. **1523** (2012) 320.

[7] CMS Collaboration, *Measurement of WW Production and Search for the Higgs Boson in pp Collisions at $\sqrt{s}$ = 7 TeV*, *Phys. Lett.* **B699** (2011) 25.

[8] ATLAS Collaboration, *Measurement of the WW cross section in $\sqrt{s}$= 7 TeV pp collisions with the ATLAS detector and limits on anomalous gauge couplings*, *Phys. Lett.* **B712** (2012) 289-308, arXiv:1203.6232 [hep-ex].

[9] A. Cisek, W. Schäfer and A. Szczurek, *Production of Z^0 bosons with rapidity gaps: exclusive photoproduction in γp and p p collisions and inclusive double diffractive Z^0*, *Phys. Rev.* **D80** (2009) 074013.

[10] A. Kulesza and W.J. Stirling, *Like-Sign W Boson Production at the LHC as a Probe of Double Parton Scattering*, *Phys. Lett.* **B475** (2000) 168.

[11] J.R. Gaunt, Ch.-H. Kom, A. Kulesza and W.J. Stirling, *Same-sign W pair production as a probe of double parton scattering at the LHC*, arXiv:1003.3953 [hep-ph].

[12] J.R. Gaunt, Ch.-H. Kom, A. Kulesza and W.J. Stirling, *Probing double parton scattering with leptonic final states at the LHC*, arXiv:1110.1174 [hep-ph].

[13] W. Krasny and W. Płaczek, *The LHC excess of four-lepton events interpreted as Higgs-boson signal: background from Double Drell–Yan process*, *Acta Physica Polonica***B 45** (2014) 71, arXiV:1305.1769 [hep-ph].

[14] M.G. Ryskin and A.M. Snigirev, *Fresh look at double parton scattering*, *Phys. Rev.* **D83** (2011) 114047.

[15] B. Blok, Yu. Dokshitzer, L. Frankfurt and M. Strikman, *Perturbative QCD correlations in multi-parton collisions*, arXiv:1306.3763.

[16] CMS Collaboration, *Study of exclusive two-photon production of W^+W^- in pp collisions at $\sqrt{s}$ = 7 TeV and constraints on anomalous quartic gauge couplings*, *JHEP 07* (2013) 116, arXiv:1305.5596 [hep-ex].

[17] D0 Collaboration, *Search for anomalous quartic $WW\gamma\gamma$ couplings in dielectron and missing energy final states in ppbar collisions at $\sqrt{s}$ = 1.96 TeV*, *Phys. Rev.* **D 88**, 012005 (2013), arXiv:1305.1258 [hep-ex].

[18] A. Bierweiler, T. Kasprzik, H. Kühn and S. Uccirati, *Electroweak corrections to W-boson pair production at the LHC*, *JHEP 1211* (2012)093;
A. Bierweiler, T. Kasprzik and J.H. Kühn, *Vector-boson pair production at the LHC to $O\alpha^3$ accuracy*, arXiv:1305.5402;
J. Baglio, Le Duc Ninh and M.M. Webber, *Massive gauge boson pair production at the LHC: a next-to-leading order story*, *Phys. Rev.* **D 88**, 113005 (2013), arXiv:1307.4331.

[19] G. Aad, et al. [ATLAS Collaboration], *Observation of a new particle in the search for the Standard Model Higgs boson with the ATLAS detector at the LHC*, *Phys. Lett.* **B716**, 1 (2012); [ATLAS Collaboration], *A particle consistent with the Higgs Boson observed with the ATLAS Detector at the Large Hadron Collider*, *Science* **338**, 1576 (2012).

[20] S. Chatrchyan, et al. [CMS Collaboration], *Observation of a new boson at a mass of 125 GeV with the CMS experiment at the LHC*, *Phys. Lett.* **B716**, 30 (2012); S. Chatrchyan, et al. [CMS Collaboration], *A new boson with a mass of 125-GeV observed with the CMS experiment at the Large Hadron Collider*, *Science* **338**, 1569 (2012).

[21] J. Ohnemus, *Order α_s calculation of hadronic $W^{+-}Z$ production*, *Phys. Rev.* **D44** (1991) 3477;
S. Frixione, P. Nason and G. Ridolfi, *Strong corrections to W Z production at hadron colliders*, *Nucl. Phys.* **B383** (1992) 3;
L.J. Dixon, Z. Kunszt and A. Signer, *Helicity Amplitudes for $\mathcal{O}(\alpha_s)$ Production of $W^+W^-, W^{+-}Z, ZZ, W^{+-}\gamma$, or $Z\gamma$ Pairs at Hadron Colliders*, *Nucl. Phys.* **B531** (1998) 3;
J.M. Campbell, R.K. Ellis, *Update on vector boson pair production at hadron colliders*, *Phys. Rev.* **D60** (1999) 113006.

[22] A. Denner, S. Dittmaier and R. Schuster, *Radiative Corrections to $\gamma\gamma$ to W^+W^- in the Electroweak Standard Model*, *Nucl. Phys.* **B452** (1995) 80.

[23] M. Drees and D. Zeppenfeld, *Production of supersymmetric particles in elastic ep collisions*, *Phys. Rev.* **D39** (1989) 2536.

[24] D.A. Dicus, C. Kao and W. Repko, *Gluon production of gauge bosons*, *Phys. Rev.* **D36** (1987) 1570;

E.N. Glover and J. van der Bij, *Vector Boson Pair Production Via Gluon Fusion*, *Phys. Lett.* **B219** (1989) 488;
E.N. Glover and J. van der Bij, *Z Boson Pair Production Via Gluon Fusion*, *Nucl. Phys.* **B321** (1989) 561.

[25] E. Eichten, L. Hinchliffe, K. Lane, C. Quigg, *Supercollider physics*, *Rev. Mod. Phys.* **56** (1984) 579.

[26] M. Drees, R.M. Godbole, M. Nowakowski and S.D. Rindani, $\gamma\gamma$ *Processes at High Energy pp Colliders*, *Phys. Rev.* **D50** (1994) 2335.

[27] A.D. Martin, R.G. Roberts, W.J. Stirling, R.S. Thorne, *Parton distributions incorporating QED contributions*, *Eur.Phys.J.***C39**:155-161,2005.

[28] G. Kubasiak and A. Szczurek, *Inclusive and exclusive diffractive production of dilepton pairs in proton-proton collisions at high energies*, *Phys. Rev.* **D84** (2011) 014005.

[29] M. Łuszczak, R. Maciuła and A. Szczurek, *Subdominant terms in the production of $c\bar{c}$ pairs in proton-proton collisions*, *Phys. Rev.* **D84** (2011) 114018.

[30] A. Aktas *et al.* [H1 Collaboration], *Measurement and QCD Analysis of the Diffractive Deep-Inelastic Scattering Cross Section at HERA*, *Eur. Phys. J. C* **48**, 715 (2006), [arXiv:hep-exp/0606004].

[31] V.A. Khoze, A.D. Martin and M.G. Ryskin, *Soft diffraction and the elastic slope at Tevatron and LHC energies: A MultiPomeron approach*, *Eur. Phys. J.* **C18** (2000) 167.

[32] U. Maor, *The Interplay between Data and Theory in Recent Unitarity Models*, *AIP Conf. Proc.* **1105** (2009) 248.

[33] J. R. Gaunt, R. Maciula, A. Szczurek, *Conventional versus single-ladder-splitting contributions to double parton scattering production of two quarkonia, two Higgs bosons and $c\bar{c}c\bar{c}$*, arXiv:1407.5821.

[34] M. Łuszczak, R. Maciuła and A. Szczurek, *Production of two $c\bar{c}$ pairs in double-parton scattering*, *Phys. Rev.* **D85** (2012) 094034.

[35] R. Maciuła and A. Szczurek, *Production of $c\bar{c}c\bar{c}$ in double-parton scattering within kt-factorization approach- meson-meson correlations*, *Phys. Rev.* **D87** (2013) 074039.

[36] CMS Collaboration, *Observation of a diffractive contribution to dijet production in proton-proton collisions at $\sqrt{s}$ = 7 TeV*, *Phys. Rev.***D 87** (2013) 012006, arXiv:1209.1805.

[37] R.D. Ball, V. Bertone, S. Carrazza, L. Del Debbio, S. Forte, A. Guffanti, N.P. Harltland and J. Rojo, *Parton distributions with QED corrections*, arXiv:1308.0598.